Annals of Biomedical Engineering, Vol. 30, pp. 946–960, 2002
Printed in the USA. All rights reserved.

0090-6964/2002/30(7)/946/15/$15.00

Dynamic Modeling and Simulation of Nitric Oxide Gas Delivery to Pulmonary Arterioles

HOON SUNG JEH[1] and STEVEN C. GEORGE[1,2]

[1]Department of Chemical Engineering and Materials Science, [2]Center for Biomedical Engineering, University of California–Irvine, Irvine, CA

(Received 6 September 2001; accepted 26 June 2002)

Abstract—Nitric oxide (NO) is an effective dilator of the pulmonary arterial circulation for treatment of pulmonary hypertension. A wide range of inhalation breathing patterns and concentrations have proven effective, but the mechanisms underlying this variability are not known. We have developed a dynamic model of NO gas inhalation, which considers inhalation, diffusion, and reaction of NO in the pulmonary arteriolar region, and also considers disease progression. The response of the system (mean concentration of NO in the smooth muscle, $\overline{c}_{sm}$) is characterized using an overall transfer function. The model is used to simulate previously published experimental NO gas inhalation patterns in which a short pulse of 100 ppm of NO gas was applied at the start of inhalation. Our model predicts the clinically effective $\overline{c}_{sm}$ to be 0.22–0.41 nM, which is far smaller than the equilibrium dissociation constant of soluble guanylyl cyclase previously estimated *in vitro* ($<$250 nM) and theoretically (23 nM). We conclude that the clinically effective $\overline{c}_{sm}$, and the overall transfer function may be useful in the design of new NO-delivery strategies for the treatment of pulmonary hypertension. © *2002 Biomedical Engineering Society.* [DOI: 10.1114/1.1507327]

Keywords—NO, Pulmonary hypertension, Guanylyl cyclase, Smooth muscle.

INTRODUCTION

Ever since nitric oxide (NO) was discovered to be a key vasorelaxant (endothelium-derived relaxing factor or EDRF),[26] potential therapeutic applications have been aggressively pursued both experimentally[17,20,21,34,37] and theoretically.[5,27,31] NO gas inhalation has proven an effective therapy for pulmonary hypertension (PH), due to the dilation of the small arteries (arterioles) in the pulmonary circulation of the lungs. NO is thought to diffuse across the adventitial tissue barrier and activate soluble guanylate cyclase (sGC) in the vascular smooth muscle of well-ventilated regions of the lungs in patients with endothelial dysfunction.[7,11,25] Excess NO is scavenged by hemoglobin in the red blood cells.[4] Thus, NO gas inhalation avoids systemic hypotension, a significant disadvantage of other vasodilators (i.e., prostacyclin) used in the treatment of PH.[22,24,32]

Currently, many different inhalation patterns and NO gas concentrations have proven effective,[15,16,37] however, the underlying mechanisms (e.g., effective concentration of NO in the smooth muscle) and fate (e.g., loss of NO to hemoglobin) of the inhaled NO are poorly understood. The NO-sGC reaction can be confined to the pulmonary arterioles; thus, a well-defined model describing inhalation, diffusion, and reaction of inhaled NO can be developed to improve our understanding of the mechanisms underlying the clinically observed pulmonary vasodilation.

This study presents the first dynamic model of NO gas inhalation and delivery to the pulmonary circulation. Our goals are to determine the minimum number of parameters necessary to describe the system, simulate experimental inhalation patterns that have proven effective clinically, and determine the parameters that have the largest impact on the concentration of NO in the smooth muscle. This type of analytical framework will not only provide insight into understanding existing experimental data, but should prove useful in designing future therapeutic strategies for delivering NO to pulmonary arterioles.

METHODS

Model Development

Inhalation of exogenous NO gas is through the upper respiratory tract and conducting airways to alveolar region of the lungs. Once present in the alveolar region, NO diffuses freely into the surrounding tissue. From there, it crosses the alveolar membrane and enters the capillary nets where it reacts with hemoglobin. Simultaneously, a relatively small fraction of the inhaled NO diffuses across the adventitial connective tissue to reach the smooth muscle of the pulmonary arterioles. If exogenous NO is delivered continuously in the inspired gas,

Address correspondence to Steven C. George, MD, Ph.D., Department of Chemical Engineering and Materials Science, 916 Engineering Tower, University of California–Irvine, Irvine, CA 92697-2575. Electronic mail: scgeorge@uci.edu

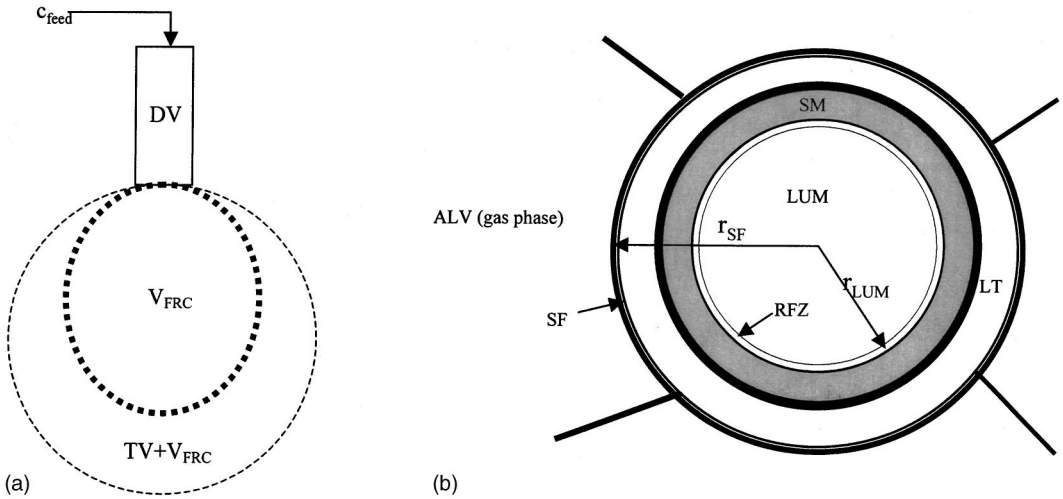

FIGURE 1. (a) Model for alveolar NO gas concentration responding to feed gas concentration based on balloon and stick model. Quick and complete mixing is assumed in the alveolar region, which is beyond convection–diffusion front. c_{feed}: feed NO concentration; V_{FRC}: alveolar functional residual capacity; TV: tidal volume; DV: dead-space volume. (b) Cross section of small pulmonary arteriole. LUM: lumen; RFZ: red blood cell (rbc) free zone; SM: smooth muscle cell; LT: lung adventitial tissue; SF: surfactant layer; ALV: alveolar region (gas phase).

we surmise a steady state alveolar concentration is eventually attained, which can then serve as a boundary condition for diffusion into the arteriole smooth muscle. Thus, our dynamic model separates the system into two components: (1) NO gas inhalation from the exogenous air source to the alveolar gas (a macroscopic stage referred to as *Gas Inhalation*), and (2) molecular diffusion from the alveolar gas to the pulmonary arteriolar smooth muscle (a microscopic stage referred to as *Arteriolar Diffusion*).

Gas Inhalation

Figure 1(a) depicts a simplified macroscopic lung model in which the pulmonary respiratory system is divided into two parts: (1) the conducting airways including trachea and bronchioles, and (2) the respiratory region including the respiratory bronchioles and alveoli. Although the airways are somewhat flexible, conducting airway volume changes are small during tidal breathing and relative to the volume changes in the alveolar region. Thus, the conducting airways are considered rigid tubes of constant volume consistent with prior models of the pulmonary gas transport.[35] Minimal exogenous NO exchange between the gas phase and the tissue phase occurs in the airway compartment due to low NO solubility; thus, the airways are considered dead space, and the volume will be referred to as dead-space volume (DV).

The volume of the alveolar or respiratory region varies as it expands during inhalation and contracts during exhalation. At the end of tidal expiration, the volume of the lungs (respiratory region and dead space, DV) is the functional reserve capacity (FRC). The volume of the respiratory region or alveolar fraction (V_{FRC}) is then FRC-DV. The expanded lung volume at the end of inhalation is the volume increased from V_{FRC} by TV (tidal volume). Once present in the alveolar region, NO can diffuse into the surrounding capillary blood. The dominant mechanism of transport in the airways and the respiratory region is convection and diffusion, respectively. The convection-diffusion front[35] is assumed to be at the border of the two regions. The respiratory region is assumed to be instantaneously well-mixed (no spatial concentration gradients). Thus, there are four input parameters during gas inhalation: breathing frequency (f), DV, TV, and FRC.

A mass balance for NO in the alveolar region during inhalation and expiration results in the following governing nondimensional differential equations as derived in the Appendix:

inhalation:

$$\frac{d\hat{c}_{alv}}{d\hat{t}} = \frac{1}{\hat{V}}\left((\hat{c}_{feed} - \hat{c}_{alv})\frac{d\hat{V}}{d\hat{t}} - \frac{D_{L,NO}}{V_{FRC}(1+V_r)f}\hat{c}_{alv} \right), \quad (1)$$

exhalation:

$$\frac{d\hat{c}_{alv}}{d\hat{t}} = -\frac{D_{L,NO}}{V_{FRC}(1+V_r)f}\frac{\hat{c}_{alv}}{\hat{V}}, \quad (2)$$

where $\hat{V}$ is dimensionless alveolar volume $[(V)/V_{FRC} + TV]$, $\hat{c}_{feed}$ is dimensionless concentration of NO enter-

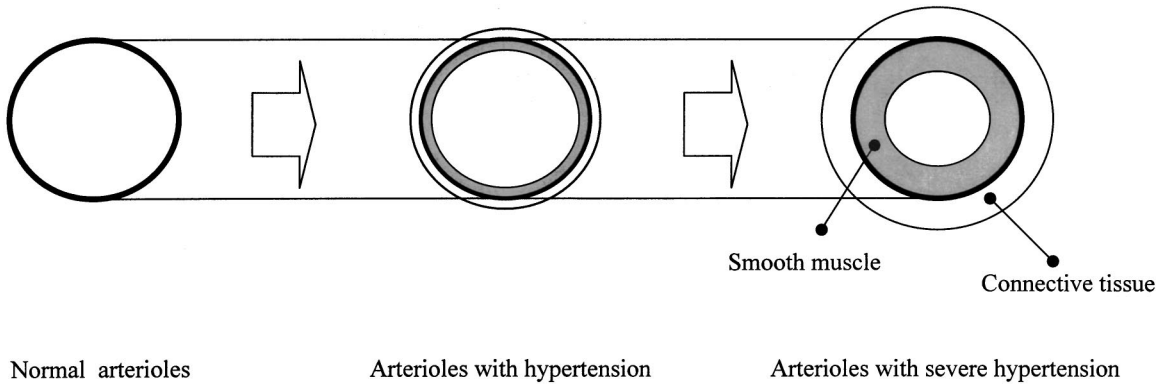

FIGURE 2. Model progression of pulmonary hypertension. (——): precursor cells (pericytes and intermediate cells), (■): smooth muscle cell region (SM), (□): lung adventitial tissue (LT).

ing to alveolar region, $\hat{c}_{alv}$ is dimensionless NO concentration in the alveolar region (c_{alv}/c_{feed}), $\hat{t}$ is dimensionless time $[t/(1/f)=tf]$, $D_{L,NO}$ is the alveolar diffusing capacity ($\mathrm{mol\,s^{-1}\,M^{-1}}$), f is breathing frequency ($\mathrm{s^{-1}}$), and V_r is ratio of TV to V_{FRC}, respectively. $D_{L,NO}$ was initially set equal to $48\,V^{2/3}$ as previously described[29] where V is alveolar volume expressed in liters, and $D_{L,NO}$ is expressed in $\mathrm{ml\,min^{-1}\,mm\,Hg^{-1}}$ (STPD); then, $D_{L,NO}$ was converted to the units $\mathrm{mol\,s^{-1}\,M^{-1}}$ for the calculations.

Arteriolar Diffusion

Figure 1(b) shows the microscopic anatomy of an arteriole having a smooth muscle cell layer and a connective tissue layer on the vessel wall. Pulmonary hypertension is directly related to the function of the muscle layers in the arterioles.[23] Previous investigators have demonstrated that both the smooth muscle cell and adventitial layers thicken approximately equally during the progression of pulmonary hypertension.[10,28,33] Figure 2 depicts disease development. Normal small (diameter $<100\ \mu$m) arterioles (top) have a single thin layer with a few pericytes or intermediate cells comprising the vessel walls, and negligible smooth muscle.[10] During the progression of pulmonary hypertension, a smooth muscle cell layer forms from the proliferation of precursor cells on the wall, with the simultaneous thickening of the adventitia.[33] Horsefield reported the morphometry of the pulmonary circulation and dimensions of the arteries prior to the capillary bed of the alveoli in a human body.[12] The report demonstrated that the small arterioles could be characterized by three populations of progressively increasing diameters: 34, 54, and 86 μm diameter. Thus, our model will consider these three different diameters as representative sized-vessels involved in pulmonary hypertension. Although larger arteries could cause pulmonary hypertension, the smallest arterioles are most accessible to NO gas inhalation by diffusion.

In the lumen of the arteriole, NO molecules are scavenged by hemoglobin in red blood cells.[1] The precise

TABLE 1. Parameter ranges used in the modeling and simulation.

Parameter	Range	Control value	References
FRC	2.5–5 L	2.7 L	29, 35
TV	350–1000 ml	500 ml	35
DV	150–200 ml	200 ml	29, 35
f	0.2–0.25 $\mathrm{s^{-1}}$	0.2 $\mathrm{s^{-1}}$	35
$D_{NO,w}$	3300–5160 $\mu\mathrm{m^2\,s^{-1}}$	3300 $\mu\mathrm{m^2\,s^{-1}}$	17, 31, 36
k_h	15–230,000 $\mathrm{s^{-1}}$	1280 $\mathrm{s^{-1}}$	31
Diameter	34, 54, 86, 138 μm	34 μm	13
Muscle thickness	6–77 μm	6 μm	10, 23, 28, 32
Connective tissue thickness	6–100 μm	6 μm	10, 23, 28, 32
Vr	0.07–0.4	0.185	
Da	2.6×10^{-6}–0.026	0.00026	
$\hat{r}_{LUM}$	0.2–0.96	0.227	

FRC: functional residual capacity, TV: tidal volume, DV: dead space volume, f: breathing frequency, $D_{NO,w}$: diffusivity of NO in water phase; k_h: reaction constant of hemoglobin-NO reaction, Vr: ratio of TV to V_{FRC}, Da: Damkohler number, $\hat{r}_{LUM}$: dimensionless lumen radius.

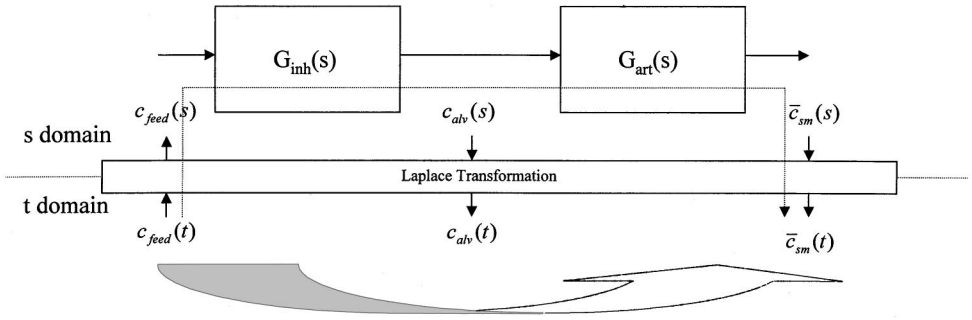

FIGURE 3. Strategy for dynamic simulation by transfer functions in s domain. Calculation in s-domain facilitate estimation of the output to various input functions. G_{inh}: transfer function for NO gas inhalation, G_{art}: transfer function for arterial region, $c_{feed}(s)$: feed NO concentration; C_{alv}: alveolar NO concentration, $\bar{c}_{sm}$: mean NO concentration in smooth muscle cell region.

fate of NO in blood in terms of diffusion and chemical association with hemoglobin remains an active area of research. For example, NO can bind to cysteine residues[9,14] as well as the heme center of hemoglobin. In addition, a significant diffusion barrier exists in either the plasma[18] or red blood cell membrane.[30] Nonetheless, consumption of NO by hemoglobin remains rapid relative to the time scale of gas inhalation. For simplicity, the reaction kinetics is assumed to be first order, and the reaction constant spans a wide range as reported by previous investigators (Table 1). At the border of the lumen and inner side of the vessel wall, a red blood cell free zone (RFZ) is introduced consistent with previous reports.[4,31] NO consumption is neglected in the RFZ, and only radial diffusion is considered. As in the red blood cell free zone (RFZ), NO consumption was neglected in the lung adventitia tissue (LT) region. A thin surfactant layer outside the vessel wall contacts the outer gas phase, and a gas–liquid equilibrium state is established between the alveolar gas phase and the aqueous phase of the surfactant layer. The gas–liquid equilibrium is characterized by a partition coefficient between two phases, and the value was taken as 1.6 nM of NO in water phase per 1 ppm of NO in gas phase.[13] The diffusivity of NO in the tissue layers is assumed to be constant and equal to the diffusivity of NO in water. Thickened tissue, as would occur in pulmonary hypertension, is expected to alter the dimensions of the tissue, but not expected to alter the diffusivity.

The coordinates of the arteriole are assumed cylindrical and end effects are neglected. Based on published half-lives of NO in tissue as well as reaction rate expressions for NO with substrates such as superoxide, soluble guanylate cyclase, and oxygen, we found that exogenous NO consumption by chemical reaction was negligible relative to the rate of diffusion. The ratio of the consumption rate (product of reaction rate per unit volume and volume of tissue, moles s^{-1}) by chemical reaction with oxygen or with soluble guanylate cyclase in smooth muscle[8,19] to the rate of NO diffusion across the wall (product of diffusion flux and surface area, moles s^{-1}) was less than 10^{-3} and 10^{-4} order, respectively (data not shown). Hence, the governing equations were simplified. The mass balance for NO in the arteriolar wall then reduces to the following dimensionless differential equations:

$$\frac{\partial \hat{c}_{\text{art}}}{\partial \hat{t}} = \text{Da}\frac{1}{\hat{r}}\frac{\partial}{\partial \hat{r}}\left(\hat{r}\frac{\partial c_{\text{art}}}{\partial \hat{r}}\right) - \hat{c}_{\text{art}} \quad \text{at LUM,} \tag{3}$$

$$\frac{\partial \hat{c}_{\text{art}}}{\partial \hat{t}} = \text{Da}\frac{1}{\hat{r}}\frac{\partial}{\partial \hat{r}}\left(\hat{r}\frac{\partial c_{\text{art}}}{\partial \hat{r}}\right) \quad \text{at RFZ, SM, LT, and SF,} \tag{4}$$

$$\hat{c}_{\text{art}}(1,\hat{t}) = 1,$$

$$\frac{\partial \hat{c}_{\text{art}}}{\partial \hat{t}}(0,\hat{t}) = 0, \quad \text{for boundary conditions,} \tag{5}$$

$$\hat{c}_{\text{art}}(\hat{r},0) = 0,$$

where $\hat{c}_{\text{art}} = c_{\text{art}}/c_{\text{sf}}, \hat{r} = (r)/r_{\text{SF}}, \hat{t} = [t/(1/k_h)]$, and Da is $D_{\text{NO},w}/r_{\text{SF}}^2 k_h$.

The concentration is assumed to be continuous across the boundary at $\hat{r} = \hat{r}_{\text{LUM}}$. $D_{\text{NO},w}$ is the diffusion coefficient of NO in the aqueous phase, r_{SF} is the radius of surfactant layer, and k_h is the hemoglobin reaction constant, respectively. The governing equations can be fully characterized by only two dimensionless input parameters: (1) Da is a type of Damkohler number which represents the ratio of the rate of diffusion to the rate of chemical consumption by hemoglobin in the blood, and (2) $\hat{r}_{\text{LUM}}$ is a dimensionless parameter determining the boundary condition.

Model Solution

With the governing equations and boundary conditions, the numerical solution for the dynamic responses of NO concentration of the arteriole region was obtained by finite element integration and nonlinear equation solving with Mathematica®. Figure 3 describes our general solution strategy. Our goal is to calculate or predict the NO concentration in the smooth muscle cells $[c_{sm}(t)]$ of arterioles responding to a feed concentration of the gas $[c_{feed}(t)]$. In order to accomplish this, we need to know the NO gas concentration in the alveolar region around the arteriole $[c_{alv}(t)]$. In the ordinary t domain, the concentration profiles can be calculated for each input function $c_{feed}(t)$ by solving the differential equations governing the system (the wide arrow). To provide a more robust solution, we utilize the Laplace transformation and the definition of a transfer function, $G(s)$:

$$G(s)=\frac{\text{out}(s)}{\text{in}(s)}. \tag{6}$$

In the s domain, any output, $[\text{out}(s)]$, responding to any arbitrary input $[\text{in}(s)]$ can be algebraically calculated by simple multiplication of $G(s)$ and $\text{in}(s)$. The inverse-transformation of $\text{out}(s)$ allows one to obtain $\text{out}(t)$ in the time domain (t domain).

The gas inhalation step can also be modeled as in Fig. 3. The alveolar concentration is independent of the small region of arteriole diffusion. Thus, we assumed that the gas concentration is solely determined by the consumption through capillary nets on alveoli, and is therefore uncoupled from the second step. When the second output variable does not affect the first output variable, the system is a noninteracting system, and the two transfer functions can be multiplied to form the overall transfer function that governs the overall process:

$$G_{inh}(s)=\frac{c_{alv}(s)}{c_{feed}(s)}$$

and

$$G_{art}(s)=\frac{\overline{c}_{sm}(s)}{c_{alv}(s)}, \tag{7}$$

so

$$G_{tot}(s)=\frac{\overline{c}_{sm}(s)}{c_{feed}(s)}=G_{inh}(s)G_{art}(s) \tag{8}$$

and

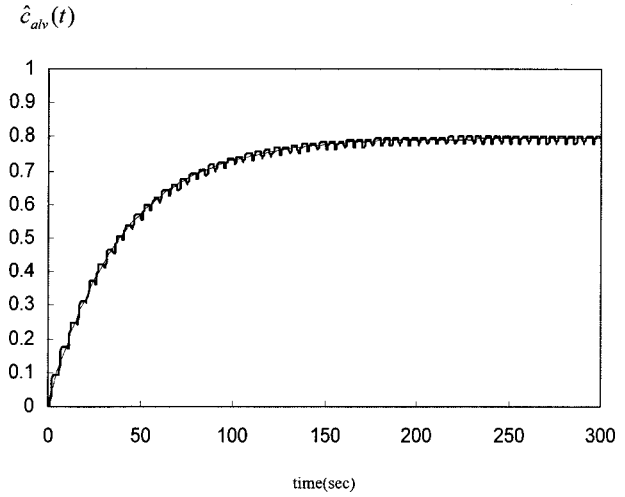

FIGURE 4. Calculated NO concentration in alveolar gas phase responding to a unit step input change of c_{feed}. Breathing frequency of 0.2/s, V_{FRC} of 2.7 L and TV of 0.5 L were used.; $\hat{c}_{alv}$: dimensionless alveolar NO concentration (c_{alv}/c_{feed}). The smooth line indicates data fit of first-order response.

$$\overline{c}_{sm}(t)=L^{-1}[\overline{c}_{sm}(s)]=L^{-1}[G_{tot}(s)c_{feed}(s)]. \tag{9}$$

Therefore, the mean (over radial position) concentration in the smooth muscle, $\overline{c}_{sm}(t)$, can be calculated for any arbitrary input given, $c_{feed}(s)$, if the total transfer function of the system, $G_{tot}(s)$, is known, and the necessary inverse transformation (L^{-1}) to the t domain can be performed.

RESULTS

$G_{inh}(s)$

$\hat{c}_{alv}(t)$ was calculated by solving Eqs. (1) and (2) following a step change in $c_{feed}(t)$. Lung volumes representative of an adult human lung were utilized (DV $=200$ ml, FRC$=2700$ ml, TV$=500$ ml). f was set to $0.2\ s^{-1}$. The response for the step input change in c_{feed} (Fig. 4) demonstrates typical first-order saturation kinetics:

$$\hat{c}_{alv}(t)=g_{inh}(1-e^{-t/\tau_{inh}}), \tag{10}$$

where g_{inh} is the gain or steady state response of the inhalation step defined physically as the ratio of the steady state alveolar concentration to the feed concentration. $G_{inh}(s)$ can then be derived by the definition and theorems of the Laplace transformation:

$$G(s)=\frac{\text{out}(s)_{step}}{\text{in}(s)_{step}}=\frac{\text{out}(s)_{step}}{1/s}=s\,\text{out}(s)_{step}=L[\text{out}(t)'_{step}]. \tag{11}$$

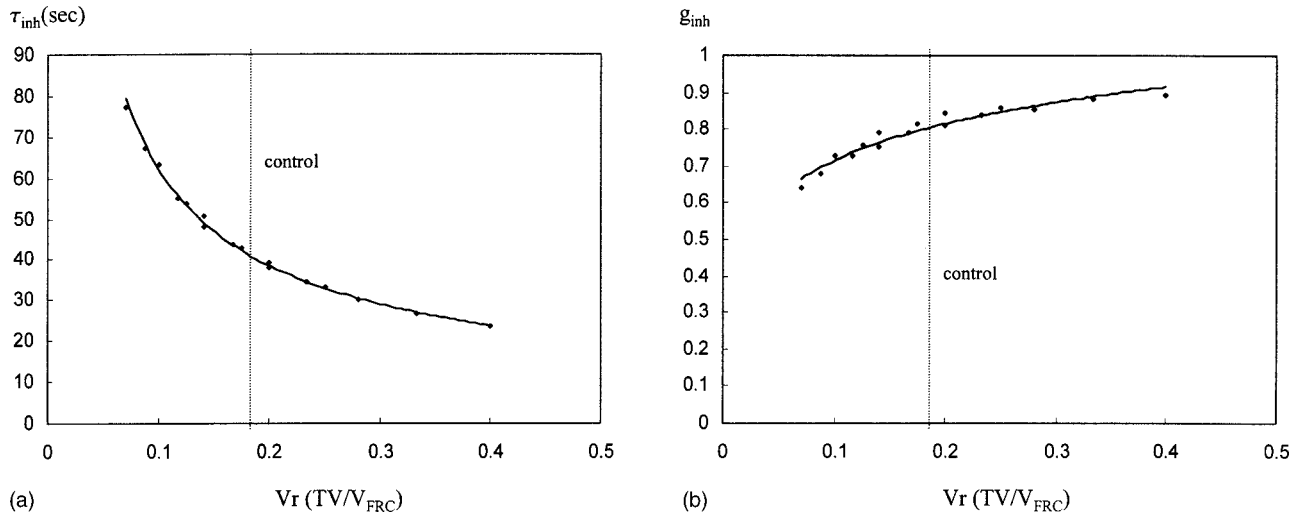

FIGURE 5. Dependence of time constant (a) and gain (b) of inhalation step on dimensionless volumetric parameters Vr(TV/V_{FRC}); dashed lines indicate the values based on the control values in Table 1.

This means that the Laplace transform of the differential function of the output function responding to a unit step input function is simply the transfer function of the system. Therefore,

$$G_{\text{inh}}(s) = L[g_{\text{inh}}(1-e^{-t/\tau_{\text{inh}}})'] = L[(g_{\text{inh}}/\tau_{\text{inh}})e^{-t/\tau_{\text{inh}}}] = \frac{g_{\text{inh}}}{\tau_{\text{inh}}s+1}, \quad (12)$$

where g_{inh} and τ_{inh} are the gain and time constant of the transfer function, respectively. The value of the constants τ_{inh} were obtained by linear regression of the simulated results on a semilog graph. The dimensionless parameter in the governing equation, V_r ($=\text{TV/V}_{\text{FRC}}$) impacts τ_{inh} as demonstrated in Fig. 5(a). In contrast, the steady state response (g_{inh}: gain) of $G_{\text{inh}}(s)$ is a weaker function of V_r as shown in Fig. 5(b):

$$G_{\text{art}}(s).$$

The concentration of NO in the smooth muscle is shown in Fig. 6. In Fig. 6(a), the time-course change of the radial NO concentration profile is shown for a control set of parameters as in Table 1. Figure 6(b) illustrates the time course for $\overline{c}_{\text{sm}}(t)$. It is evident that $\overline{c}_{\text{sm}}(t)$ also demonstrates first-order saturation behavior; thus, the solution of $\overline{c}_{\text{sm}}(t)$ can be expressed more simply as

$$\overline{\hat{c}}_{\text{sm}}(t) = g_{\text{art}}(1-e^{-t/\tau_{\text{art}}}), \quad (13)$$

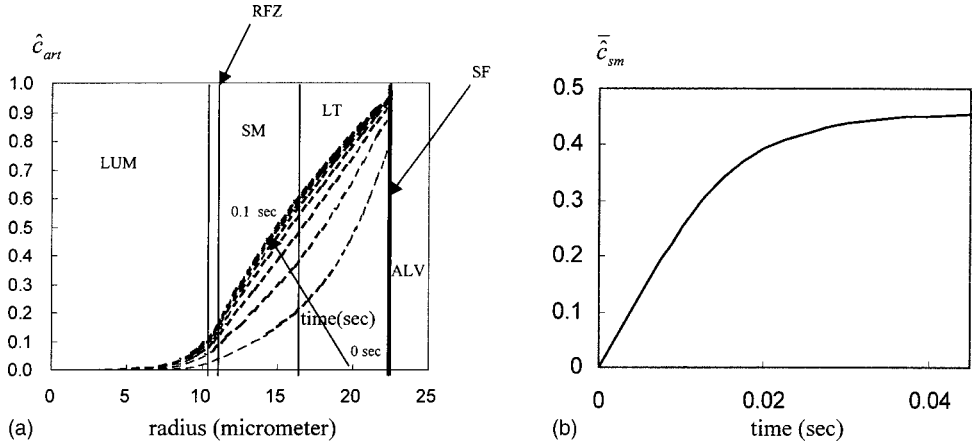

FIGURE 6. Simulation results from the arteriole model. (a) Concentration profile change in the whole arteriole region responding to a step change of alveolar NO concentration (1 ppm). The profile was obtained by solving the governing equations numerically using control parameters (Table 1). (b) Mean NO concentration change in the smooth muscle cell region.

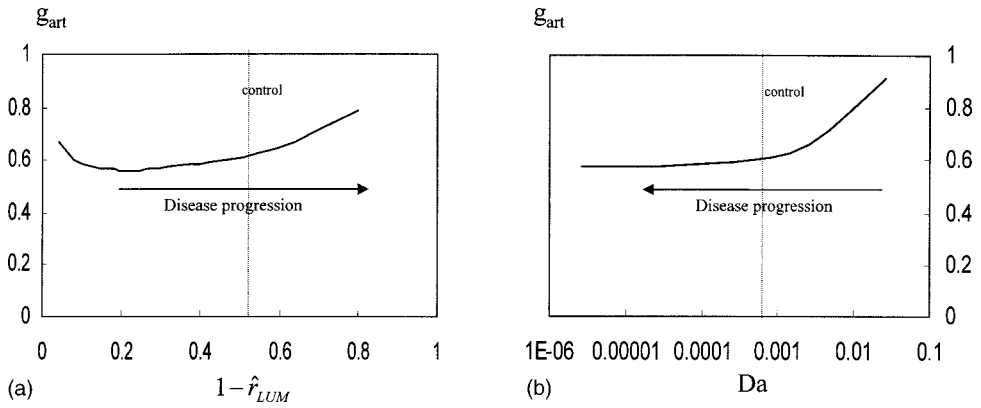

FIGURE 7. Dependence of g_{art} on the dimensionless parameters, $\hat{r}_{LUM}$ (a) and Da (b). The dashed line indicates the control value (Table 1). The ranges of values for the parameters are in Table 1.

where g_{art} is the gain or steady state response of the inhalation step defined physically as the ratio of the steady state muscular concentration to the boundary concentration at the surfactant layer (i.e., $g_{art}=\bar{c}_{sm,ss}/c_{sf,ss}=\bar{c}_{sm,ss}/hc_{alv,ss}$).

By implementing the same technique utilized to obtain $G_{inh}(s)$ [Eq. (12)], we can express $G_{art}(s)$ as

$$G_{art}(s)=L[g_{art}(1-e^{-t/\tau_{art}})']$$

$$=L[(g_{art}/\tau_{art})e^{-t/\tau_{art}}]=\frac{g_{art}}{\tau_{art}s+1}, \qquad (14)$$

where g_{art} and τ_{art} are the gain and time constant of the transfer function, respectively.

Figure 7 demonstrates the effect of the two dimensionless parameters in the governing equations (i.e., Da and $\hat{r}_{LUM}$) on the gain of the transfer function. g_{art} passes through a minimum at a value of 0.20 for $1-\hat{r}_{LUM}$ whereas it is relatively insensitive to Da for $Da<2.6\times10^{-4}$ (control value), but then increasing monotonically with increasing Da, which would increase with disease progression at constant diffusivity ($D_{NO,w}$) and reaction constant (k_h). In contrast to g_{art}, τ_{art} was relatively insensitive to changes in $\hat{r}_{LUM}$ and Da, and had a constant value of ~0.2 s—almost 3 orders of magnitude smaller than τ_{inh}:

$$G_{tot}(s).$$

From Eq. (8), the overall transfer function can be expressed as

$$G_{tot}(s)=\frac{\bar{c}_{sm}(s)}{c_{feed}(s)}=G_{inh}(s)G_{art}(s)$$

$$=\frac{g_{inh}g_{art}}{(\tau_{inh}s+1)(\tau_{art}s+1)}. \qquad (15)$$

Because the simulations demonstrated that $\tau_{inh}\gg\tau_{art}$ over a wide range of parameter values, the overall transfer function can be approximated as:

$$G_{tot}(s)\cong\frac{g_{inh}g_{art}}{\tau_{inh}s+1}, \qquad (16)$$

therefore, in the t domain, the apparent response of the system has the following form:

$$\bar{c}_{sm}=\bar{c}_{sm,ss}(1-e^{-t/\tau_{inh}}), \qquad (17)$$

where the gain, or maximum response, $\bar{c}_{sm,ss}$, is the product of both gains ($g_{inh}g_{art}$) during inhalation and diffusion whereas the dynamic response of the system is characterized solely by the time constant of inhalation, τ_{inh}.

The overall transfer function will vary depending on the values of the input parameters. Using the uncertainty in the input parameters (Table 1), we determined the

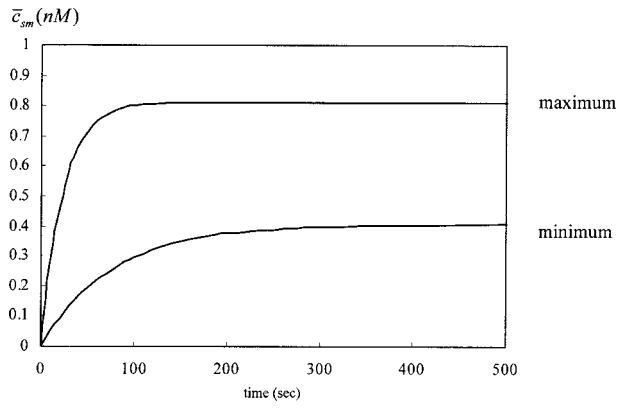

FIGURE 8. Range of the overall response to a step change from 0 to 1 ppm of NO gas inhalation. $\bar{c}_{sm}$ was calculated using the minimum and maximum overall transfer function.

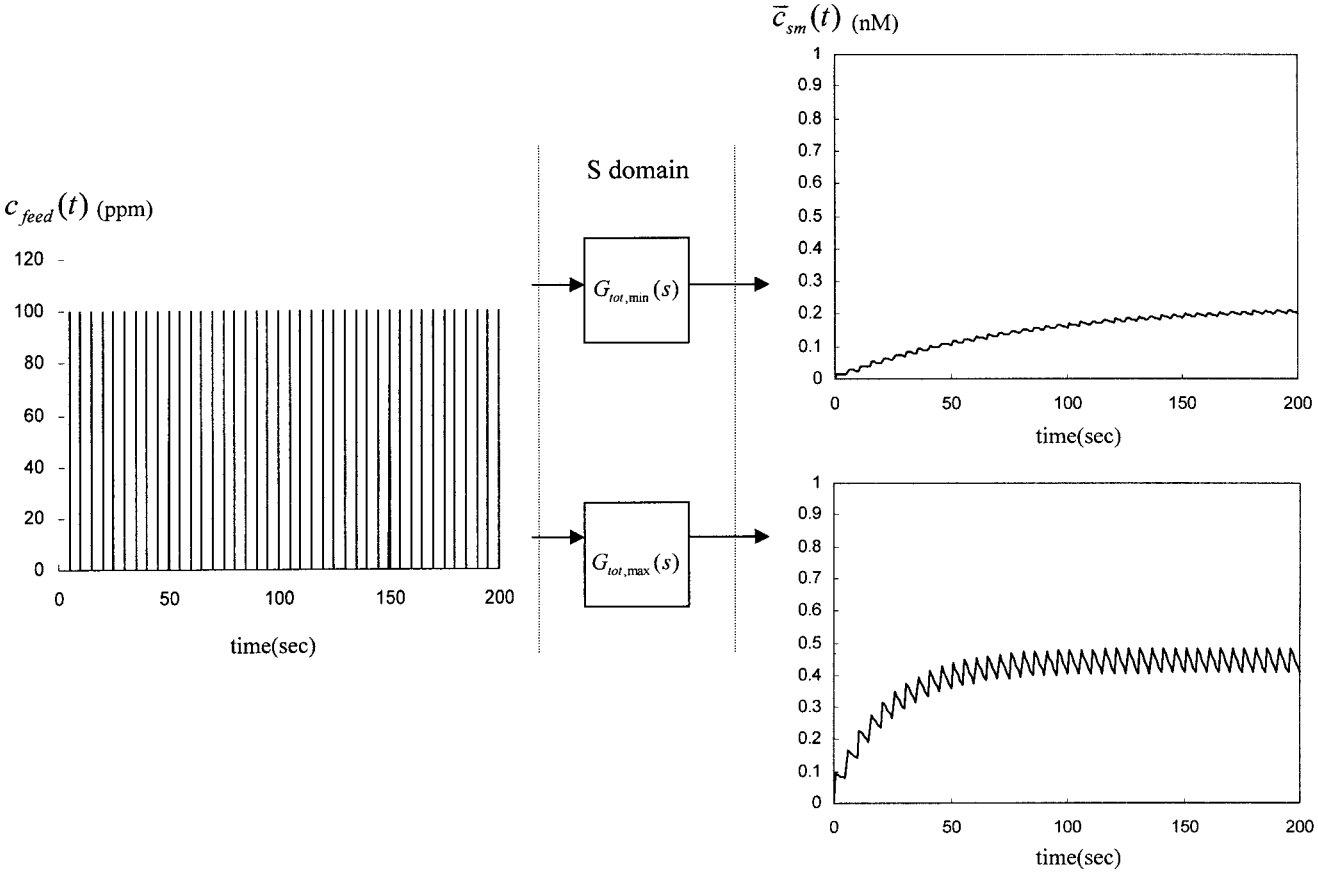

FIGURE 9. Simulation of a spike (bolus) inhalation pattern of NO gas using overall transfer functions, $G_{tot,min}(s)$ and $G_{tot,max}(s)$. The inhalation pattern is based on clinical data (Ref. 12); interspike period=5 s (at the start of each breath); peak height =100 ppm of NO, peak width=0.028 s.

minimum and maximum response ($G_{\text{tot,min}}$ and $G_{\text{tot,max}}$, respectively), of the system as characterized by the total transfer function:

$$G_{\text{tot,max}}=\frac{0.811}{23.4s+1}$$

and

$$G_{\text{tot,min}}=\frac{0.406}{77.5s+1}. \tag{18}$$

Figure 8 demonstrates the overall response of $\bar{c}_{\text{sm}}$ to a step input (1 ppm) change in $c_{\text{feed}}(t)$ using both $G_{\text{tot,min}}$ and $G_{\text{tot,max}}$. This response will be referred to as the ''response window.'' At steady state, the response window for $\bar{c}_{\text{sm,ss}}$ is 0.4–0.81 nM.

Effective Smooth Muscle Concentration ($\bar{c}_{\text{sm,eff}}$)

Previous investigators have used continuous inhalation of air mixed with trace amounts of NO gas and reported a range of 5–80 ppm to be effective for relieving pulmonary hypertension.[25,37] Thus, inhalations of these gas phase concentrations must be generating a smooth muscle concentration of NO, which is high enough to activate *s*GC. Most recently, Katayama *et al.*[15] reported the minimum amount of NO necessary for relieving pulmonary hypertension by titrating spike-inhalation patterns. They reported spike inhalations (8–38 ml) of 100 ppm NO at the start of every breath could significantly reduce pulmonary vascular resistance (PVR). From these clinical data, we can use our estimate of $G_{\text{tot}}(s)$ to estimate the minimal effective NO concentration in the smooth muscle. The form of the input function for the spike inhalation is

$$c_{\text{feed}}(s)=\sum_n \frac{e^{-(5n)s}-e^{-(5n+p)s}}{s}, \tag{19}$$

where n and p represent the breath number and the period of the NO inhalation pulse, respectively. Thus,

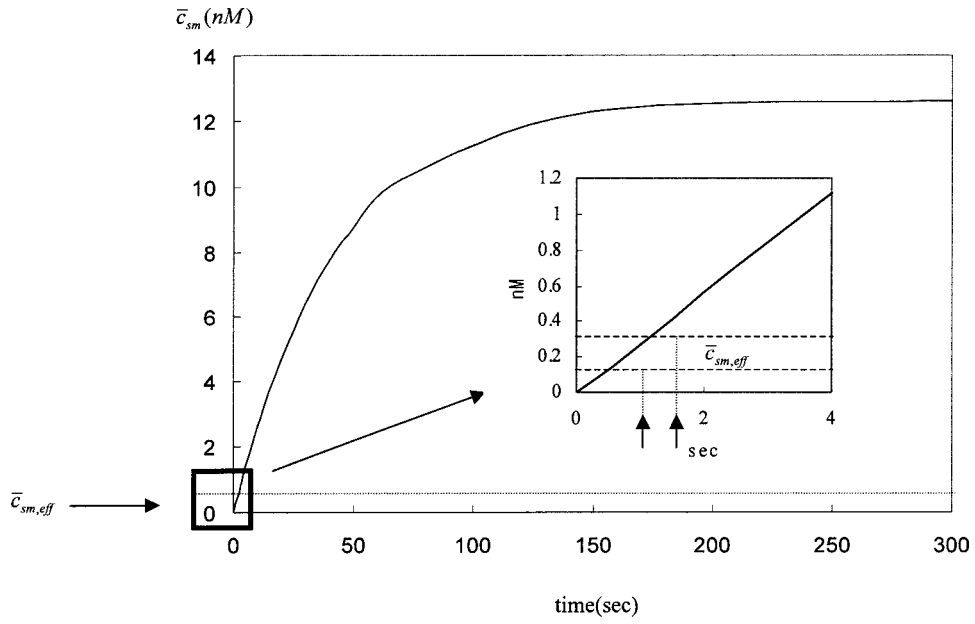

FIGURE 10. Simulation of 20 ppm continuous NO gas inhalation. The time at which $\bar{c}_{sm}$ passes the minimum effective NO concentration of smooth muscle ($\bar{c}_{sm,eff}$) is less than 2 s (inset). The dashed lines represent the model-predicted minimum effective smooth muscle concentrations, and the arrows (inset) represent the ranges of time necessary for $\bar{c}_{sm}$ to reach $\bar{c}_{sm,eff}$.

$$\bar{c}_{sm}(s) = G_{tot}(s)c_{feed}(s) = \frac{g_{inh}g_{art}}{\tau_{inh}s+1}\sum_n \frac{e^{-(5n)s} - e^{-(5n+p)s}}{s} \quad (20)$$

by the inverse Laplace transformation,

$$\bar{c}_{sm}(t) = \frac{g_{inh}g_{art}}{\tau_{inh}}\sum_n \{\tau_{inh}(e^{(5n+p-t)/\tau_{inh}} - 1)U[t-(5n+p)] + \tau_{inh}(1-e^{(5n-t)/\tau_{inh}})U(t-5n)\}, \quad (21)$$

where U represents the unit step function. Figure 9 demonstrates the form of the input function (spike inhalations) and the resulting output using both $G_{tot,max}$ and $G_{tot,min}$. A steady state is reached in 100–200 s, and the minimum effective concentration (or threshold) of NO in the smooth muscle, $\bar{c}_{sm,eff}$, is $\sim$0.22–0.41 nM.

DISCUSSION

This study has developed the first model describing the dynamics of inhalation of exogenous NO for delivery to the pulmonary arteriole region of the lungs. The primary goals of the model were to: (1) shed insight on the mechanisms underlying the wide range of effective inhaled NO concentrations demonstrated experimentally, (2) provide an estimate of the minimal effective NO concentration in the smooth muscle necessary to observe a clinical response, and (3) maintain a level of simplicity and robustness such that it could simulate the response to any unsteady state input. The latter two may be useful in the design of future therapeutic applications.

Using clinical data for titrating a minimal dose of NO gas concentration in human subjects with pulmonary hypertension,[15] our model predicts that the minimal effective NO concentration in the pulmonary arteriole smooth muscle is 0.20–0.41 nM. A continuous inhalation of NO as low as 1 ppm has also been shown to be effective for altering the pulmonary arterial pressure.[16] The model predicts a steady state mean smooth muscle concentration of 0.65 nM under this condition, but the full physiological response may take 2–3 min due to the wash-in time of the alveolar region. Previous investigators have reported levels ranging from 5 to 80 ppm as effective in relieving pulmonary hypertension which would rapidly produce NO concentrations in the smooth muscle that are larger than the required minimum. The observed decrease in PVR at inhaled concentrations of 20–80 ppm occurs rapidly (order seconds). This implies the threshold concentration might be far lower than the corresponding steady state concentration. Figure 10 plots a theoretical estimate of the mean smooth muscle concentration in response to a step change in the inhaled concentration from 0 to 20 ppm utilizing $G_{tot,min}$. Our estimation shows that the minimal effective concentration ($\sim$0.4 nM) is reached very rapidly ($<$2 s, consistent with clinical observations), but the steady state concentration (12.6 nM) is not reached for $\sim$4 min.

The model separated the exogenous delivery into two separate steps. First, the delivery or wash-in of NO gas to the alveolar region, and second, the diffusion of free NO to the pulmonary arteriole smooth muscle. Wash-in of NO to the alveolar region establishes the boundary condition for the diffusion of NO in the smooth muscle region. The time constant for the wash-in of NO (dynamic response) was several orders of magnitude larger than the time constant of diffusion in the tissue layers. Thus, tissue layers can be considered in a pseudosteady state,[5] and the dynamic response of the system is controlled entirely by the inhalation step. In contrast, the absolute *magnitude* of the response (i.e., steady state concentration in the smooth muscle) is determined by the relative loss of NO to hemoglobin in the blood. This occurs during both the inhalation phase (loss to the capillary nets surrounding the alveoli as characterized by $D_{L,\mathrm{NO}}$) and the diffusion phase (loss to the blood in the pulmonary arteriole).

Dynamic Response

The dynamic response of the system is controlled by the inhalation step. It takes $\sim 2-3$ min for the alveolar concentration to reach a steady state value following a step change in the feed or inhalation concentration. This is consistent with previous estimates for the time constant of wash-in or wash-out rates of the lungs.[6] Although we simplified the geometry of the lungs substantially by lumping the alveolar region into a single compartment, we demonstrate that τ_{inh} is 3–4 orders of magnitude larger than diffusion in the tissue region (τ_{art}). This is due to the relative volumes of the regions and the rate controlling transport mechanisms. The volume of tissue in the pulmonary arteriole is very small, and diffusion of NO, a small molecule, is very rapid. Although there are significant inhomogeneities in flow and mixing in the lungs, the potential impact will be small relative to the difference in τ_{inh} and τ_{art}. In addition, inhomogeneities tend to increase the response time of the lungs, which would only further increase the difference.

All four input parameters (TV, DV, FRC, and f) impacted τ_{inh}; however, DV and f had a smaller impact over the range presented in Table 1. τ_{inh} is determined solely by the net rate of new gas delivered to the alveolar region relative to the volume of the alveolar region. For example, as FRC increases, the volume of the alveolar region increases and thus the time constant increases. In contrast, as TV or f increases, the net rate of new gas delivered to the alveolar region increases and thus the time constant decreases.

Steady State Response

Although the dynamic response is of interest, the steady state response (gain) of the system determines the clinical response and $\overline{c}_{\mathrm{sm,eff}}$. Both steps (inhalation and tissue diffusion) significantly impact the steady state response. During inhalation, the steady state alveolar concentration is $\sim 25\%$ lower than the inhaled concentration due to loss of NO to hemoglobin in the capillaries. This is characterized by $D_{L,\mathrm{NO}}$ [Eqs. (1) and (2)], which is a positive function of lung volume as previously described. Thus, as the volume of the lung at which the tidal breathing occurs increases (increasing FRC), additional NO is lost to the capillary blood and the steady state alveolar concentration is reduced (Fig. 5).

The steady state response of the tissue diffusion step also had a significant impact on the overall steady state response. The steady state smooth muscle concentration is approximately 40% less than the alveolar concentration, but depends on both of the dimensionless input parameters and the alveolar tissue partition coefficient. We assumed that the solubility of NO in the tissue was equivalent to the solubility of NO in water. However, this is likely to underestimate the solubility due to the presence of lipids in tissue and the fact that NO is a lipophilic molecule.

The dimension of the arterioles was a dominant factor in determining NO concentration in the smooth muscle as we initially hypothesized. As pulmonary hypertension progresses, the thickness of the tissue layer (d) become larger; thus the ratio d/D [or $r_{\mathrm{SF}}-r_{\mathrm{LUM}}/(r_{\mathrm{SF}})=1-\hat{r}_{\mathrm{LUM}}$] can increase significantly. The model predicts that in the early stage of disease, the steady state response may decrease, but as the disease progresses, the steady state response may actually increase (Fig. 7). Thus, in the early stage of disease, a larger dose of NO may be required, but as the disease progresses, a smaller dose may be required to achieve the same response (or to achieve the same smooth muscle concentration). This counterintuitive concept can be explained by considering the two opposing physical phenomena impacting the smooth muscle concentration—tissue volume and blood volume. As tissue volume increases, the concentration of NO in the smooth muscle decreases due to dilution; however, as the tissue becomes larger, the volume of the blood, and thus the rate of consumption of NO by the blood, decreases which would increase the concentration.

Da represents the ratio of diffusion in the tissue to the rate of chemical consumption in the blood. For Da $<2.6\times10^{-4}$, the steady state response is independent of Da (Fig. 7). Da becomes smaller with disease progression as the radius increases, but the gain becomes insensitive to Da itself. In this case, the problem is diffusion limited, and the loss of NO that impacts the steady state response is governed completely by blood vessel wall

dimensions. For $Da > 10^{-4}$, the steady state response increases as Da increases. This can be understood by considering the case where the reaction rate constant with hemoglobin decreases. This would cause less NO to be consumed by the blood and thus increase the steady state response. For this case, the problem is no longer diffusion limited, but depends on the rate of chemical consumption.

Estimation of $\overline{c}_{sm,eff}$

The minimal effective concentration *in vivo* is essential for therapeutic design, and may vary between patients.[15] Intersubject variability might be due to different stages of the disease and accessibility of NO gas to the target arterioles. Our indirect estimation of the minimal effective NO concentration from *in vivo* data which produced a clinical response in PAP was in the range of 0.22–0.41 nM. The value is far less than estimates of the equilibrium dissociation constant for *s*GC (23–250 nM) as reported by the *in vitro* spectroscopy[27] and by theoretical analysis.[5] The equilibrium dissociation constant for *s*GC is the concentration at which 50% of the enzyme is fully activated and provides an estimate for the target therapeutic concentration. However, the concentration necessary to achieve a clinical response might be much different. For example, the pressure drop across a cylindrical tube in which the flow is laminar is inversely proportional to the radius of the tube to the fourth power,[2] thus the clinical measurement of PAP is extremely sensitive to vessel caliber. Activation of *s*GC at levels far below the equilibrium dissociation constant may provide enough change in the vessel diameter to elicit a clinical response. In addition, direct measurement of the equilibrium dissociation constant for *s*GC under *in vivo* conditions has not been reported. Experimental estimates were determined by *in vitro* spectroscopy at low temperature (10 °C) and high content of an exogenous reducing agent (5 mM dithiothreitol).[3,27] Theoretical estimates relied on extrapolation of kinetic constants to 37 °C as well as estimates of the complete kinetic mechanisms.[5]

Interestingly, some reports of NO inhalation therapies have demonstrated that continuous concentrations as low as 1 ppm of NO could relieve pulmonary hypertension.[16] Assuming aqueous solubility, the maximum concentration of NO in the smooth muscle would be only 1.6 nM, and our model predicts a steady state smooth concentration of 0.65 nM. These values are consistent with the model simulation for the spike inhalation pattern, and are still far below estimates of the equilibrium dissociation constant for *s*GC. However, NO is a lipophilic molecule, and the *in vivo* solubility, although not reported, is likely to be higher due to the presence of surfactant and other lipids in tissue.

CONCLUSION

This study has provided the first modeling study aimed at understanding quantitatively the dynamics of NO gas inhalation therapy to the pulmonary arteriole smooth muscle. The dynamic response of the system is controlled by the wash-in of NO to the alveolar region whereas the steady state response is controlled by both the loss of NO to the capillary and the arteriole blood. The analysis characterized the response of the lung by an overall transfer function, which can be used to predict the system response to any arbitrary input. Using *in vivo* clinical data, the model predicted the minimal effective smooth muscle concentration to be 0.22–0.41 nM. Knowledge of the system response and the minimal effective smooth muscle concentration might be useful in the design of new therapies aimed at delivering NO to the pulmonary arteriole smooth muscle.

ACKNOWLEDGMENTS

This work was supported by a grant from the National Institutes of Health (HL60636) and the National Science Foundation (BES-9875033).

APPENDIX

Gas Inhalation

Mass balances for NO in the alveolar region during stepwise inhalation and exhalation are:

ith inhalation:

$$\frac{d(Vc_{alv})}{dt} = \dot{V}_{in}c_{feed,alv} - D_{L,NO}c_{alv}$$

$$\text{initial condition at } t=0,\ V=V_{FRC},\ c_{alv}=c_{alv,i-1} \tag{A1}$$

ith exhalation:

$$\frac{d(Vc_{alv})}{dt} = -\dot{V}_{ex}c_{alv} - D_{L,NO}c_{alv}$$

$$\text{initial condition at } t=0,\ V=V_{FRC}+\mathrm{TV},$$

$$c_{alv}=c_{alv,i-1}, \tag{A2}$$

where V is alveolar volume (L), and

$$c_{feed,alv}\left(c_{alv,i-1} \text{ for } 0<t\leq\frac{\mathrm{DV}}{\dot{V}_{in}},\ \text{and } c_{feed} \text{ for}\frac{DV}{\dot{V}_{in}}\right)$$

is the concentration of NO entering alveolar region. At the start of ith inhaling, the previously exhaled gas in the dead space should be inhaled back prior to fresh feed gas from mouth. c_{alv} is the NO concentration in the alveolar

region (M), $D_{L,\mathrm{NO}}$ is diffusing capacity in L s^{-1}. $\dot{V}_{\mathrm{in}}$ and $\dot{V}_{\mathrm{ex}}$ are volumetric inhalation and exhalation flow rate (L s^{-1}), respectively. $D_{L,\mathrm{NO}}$ depends on alveolar volume as previously described.[29]

c_{alv}, V, and the independent variable t can be nondimensionalized with reference quantities:

$$\hat{V}=\frac{V-V_A}{V_B},\quad \hat{c}_{\mathrm{alv}}=\frac{c_{\mathrm{alv}}-c_A}{c_B},\quad \hat{t}=\frac{t}{t_{m,\mathrm{inh}}},\qquad \text{(A3)}$$

where V_A, V_B, c_A, c_B, $t_{m,\mathrm{inh}}$ are arbitrary reference quantities for making the variables nondimensional.

Substitution into the original governing equation for the inhalation step gives

$$(V_B\hat{V}+V_A)\frac{c_B d\hat{c}_{\mathrm{alv}}}{t_{m,\mathrm{inh}}d\hat{t}}+(c_B\hat{c}_{\mathrm{alv}}+c_A)\frac{V_B d\hat{V}}{t_{m,\mathrm{inh}}d\hat{t}}$$

$$=c_{\mathrm{feed,alv}}\frac{V_B d\hat{V}}{t_{m,\mathrm{inh}}d\hat{t}}-D_{L,\mathrm{NO}}(c_B\hat{c}_{\mathrm{alv}}+c_A)$$

at

$$\hat{t}=\frac{0}{t_{m,\mathrm{inh}}},\quad \hat{V}=\frac{V_{\mathrm{FRC}}-V_A}{V_B}$$

and

$$\hat{c}_{\mathrm{alv}}=\frac{0-c_A}{c_B}.\qquad \text{(A4)}$$

There are five reference quantities (c_A, c_B, V_A, V_B, and $t_{m,\mathrm{inh}}$), and thus five dimensionless groups can be specified. After letting

$$\frac{c_A}{c_B}=0,\quad \frac{c_{\mathrm{feed}}}{c_B}=1,\quad V_A=0, V_B=V_{\mathrm{FRC}}+\mathrm{TV},$$

and

$$t_{m,\mathrm{inh}}=\frac{1}{f}.\qquad \text{(A5)}$$

The dimensionless governing equation for the inhalation step reduces to

$$\frac{d\hat{c}_{\mathrm{alv}}}{d\hat{t}}=\frac{1}{\hat{V}}\left((\hat{c}_{\mathrm{feed,alv}}-\hat{c}_{\mathrm{alv}})\frac{d\hat{V}}{d\hat{t}}-\frac{D_{L,\mathrm{NO}}}{V_{\mathrm{FRC}}(1+V_r)f}\hat{c}_{\mathrm{alv}}\right)$$

at

$$\hat{t}=0,\ \hat{V}=\frac{1}{1+V_r},\ \hat{c}_{\mathrm{alv}}=\hat{c}_{\mathrm{alv},i-1},\qquad \text{(A6)}$$

where

$$\hat{t}=\frac{t}{(1/f)}=tf,\quad \hat{V}=\frac{V}{V_{\mathrm{FRC}}+\mathrm{TV}},\quad \hat{c}_{\mathrm{alv}}=\frac{c_{\mathrm{alv}}}{c_{\mathrm{feed}}},$$

and

$$V_r=\frac{\mathrm{TV}}{V_{\mathrm{FRC}}}.$$

Through the same procedure, the equation for the exhalation step is

$$\frac{d\hat{c}_{\mathrm{alv}}}{d\hat{t}}=-\frac{D_{L,\mathrm{NO}}}{V_{\mathrm{FRC}}(1+V_r)f}\frac{\hat{c}_{\mathrm{alv}}}{\hat{V}},\frac{d\hat{V}}{d\hat{t}}=-\frac{\dot{V}_{\mathrm{ex}}}{V_{\mathrm{FRC}}(1+V_r)f}$$

at

$$\hat{t}=0,\quad \hat{V}=1,\ \hat{c}_{\mathrm{alv}}=\hat{c}_{\mathrm{alv},i-1},\qquad \text{(A7)}$$

where

$$\hat{t}=\frac{t}{(1/f)}=tf,\quad \hat{V}=\frac{V}{V_{\mathrm{FRC}}+\mathrm{TV}},\quad \hat{c}_{\mathrm{alv}}=\frac{c_{\mathrm{alv}}}{c_{\mathrm{feed}}},$$

$$V_r=\frac{\mathrm{TV}}{V_{\mathrm{FRC}}},$$

and

$i=$ step number.

Arteriolar Diffusion

When the NO consumption by reaction is very small compared to the diffusion flux across the wall, the governing equations after nondimensionalizing of independent variables are:

Lumen (LUM):

$$\frac{\partial c_{\mathrm{art}}}{\partial\hat{t}}=\frac{t_{m,\mathrm{art}}D_{\mathrm{NO},w}}{r_m^2}\frac{1}{\hat{r}}\frac{\partial}{\partial\hat{r}}\left(\hat{r}\frac{\partial c_{\mathrm{art}}}{\partial\hat{r}}\right)-t_{m.\mathrm{art}}k_h c_{\mathrm{art}}.\qquad \text{(A8)}$$

Red blood cell free zone (RFZ) and wall (SM, LT, and SF):

$$\frac{\partial c_{\text{art}}}{\partial \hat{t}} = \frac{t_{m,\text{art}} D_{\text{NO},w}}{r_m^2} \frac{1}{\hat{r}} \frac{\partial}{\partial \hat{r}} \left(\hat{r} \frac{\partial c_{\text{art}}}{\partial \hat{r}} \right). \tag{A9}$$

The boundary and initial conditions are

$$c_{\text{art}}(\hat{r}=1,\hat{t}) = h c_{\text{alv}},$$

$$c_{\text{art}}(\hat{r},\hat{t}=0) = 0, \tag{A10}$$

$$\frac{\partial c_{\text{art}}}{\partial \hat{r}}(\hat{r}=0,\hat{t}) = 0,$$

where

$$\hat{t} = \frac{t}{t_{m,\text{art}}} \quad \text{and} \quad \hat{r} = \frac{r}{r_m},$$

c_{art} can be nondimensionalized with two more arbitrary reference quantities:

$$\hat{c}_{\text{art}} = \frac{c_{\text{art}} - c_A}{c_B}.$$

After substituting into Eqs. (A8), (A9), and (A10), six dimensionless groups remain in the equations:

$$\frac{\partial \hat{c}_{\text{art}}}{\partial \hat{t}} = \frac{t_{m,\text{art}} D_{\text{NO},w}}{r_m^2} \frac{1}{\hat{r}} \frac{\partial}{\partial \hat{r}} \left(\hat{r} \frac{\partial c_{\text{art}}}{\partial \hat{r}} \right) - t_{m,\text{art}} k_h \left(\hat{c}_{\text{art}} + \frac{c_A}{c_B} \right) \quad \text{at LUM}$$

$$\frac{\partial \hat{c}_{\text{art}}}{\partial \hat{t}} = \frac{t_{m,\text{art}} D_{\text{NO},w}}{r_m^2} \frac{1}{\hat{r}} \frac{\partial}{\partial \hat{r}} \left(\hat{r} \frac{\partial c_{\text{art}}}{\partial \hat{r}} \right) \quad \text{at RFZ, SM, LT, and SF}$$

$$\hat{c}_{\text{art}}(\hat{r}_{\text{SF}},\hat{t}) = \frac{c_{sf} - c_A}{c_B},$$

$$\frac{\partial \hat{c}_{\text{art}}}{\partial \hat{t}}(0,\hat{t}) = \frac{0 - c_A}{c_B},$$

$$\hat{c}_{\text{art}}(\hat{r},0) = \frac{0 - c_A}{c_B}.$$

There are four reference quantities (c_A, c_B, r_m, and $t_{m,\text{art}}$), thus four dimensionless groups can be specified. By letting

$$\frac{c_A}{c_B} = 0, \quad \frac{r_{\text{SF}}}{r_m} = 1, \quad \frac{c_{sf} - c_A}{c_B} = 1, \text{ and } k_h t_{m,\text{art}} = 1,$$

the final equations have only two dimensionless parameters in equations:

$$\frac{\partial \hat{c}_{\text{art}}}{\partial \hat{t}} = \text{Da} \frac{1}{\hat{r}} \frac{\partial}{\partial \hat{r}} \left(\hat{r} \frac{\partial c_{\text{art}}}{\partial \hat{r}} \right) - \hat{c}_{\text{art}} \text{ at LUM},$$

$$\frac{\partial \hat{c}_{\text{art}}}{\partial \hat{t}} = \text{Da} \frac{1}{\hat{r}} \frac{\partial}{\partial \hat{r}} \left(\hat{r} \frac{\partial c_{\text{art}}}{\partial \hat{r}} \right) \text{ at RFZ, SM, LT, and SF},$$

$$\hat{c}_{\text{art}}(1,\hat{t}) = 1,$$

$$\frac{\partial \hat{c}_{\text{art}}}{\partial \hat{t}}(0,\hat{t}) = 0,$$

$$\hat{c}_{\text{art}}(\hat{r},0) = 0, \tag{A11}$$

where $\hat{c}_{\text{art}} = c_{\text{art}}/(c_{\text{sf}})$, $\hat{r} = (r)/r_{\text{SF}}$, $\hat{t} = [t/(1/k_h)]$, and Da is $(D_{\text{NO},w}/r_{\text{SF}}^2 k_h)$, and the concentration is assumed to be continuous across the boundary at $\hat{r} = \hat{r}_{\text{LUM}}$. Da is a Damkohler number and $\hat{r}_{\text{LUM}}$ is the other main parameter determining the governing equations.

NOMENCLATURE

FRC	functional residual capacity
TV	tidal volume
DV	dead-space volume
V_{FRC}	alveolar FRC: FRC-DV
Vr	volume ratio: TV/FRC
$\hat{x}$	dimensionless variable of variable x
c_{sm}	NO concentration in smooth muscle cells
$\overline{c}_{\text{sm}}$	mean NO concentration in smooth muscle cells
$\overline{c}_{\text{sm,ss}}$	mean steady state NO concentration in smooth muscle cells
$\overline{c}_{\text{sm,eff}}$	minimum effective NO concentration in smooth muscle cells
c_{feed}	feed concentration of the NO gas to the mouth
$c_{\text{feed,alv}}$	feed concentration of the NO gas to the alveolar region
c_{alv}	NO concentration in the alveolar region (gas phase)

c_{art}	NO concentration in the arteriolar region (in blood and tissue)
c_{SF}	NO concentration in the surfactant layer
r_{LUM}	radius of vessel lumen
$G(s)$	transfer function
$\text{in}(s)$	input function in s domain
$\text{out}(s)$	output function in s domain
$G_{inh}(s)$	transfer function for gas inhalation
$G_{art}(s)$	transfer function for arteriole region
$G_{tot}(s)$	overall transfer function
$\text{in}(s)_{step}$	unit step input function
$\text{out}(s)_{step}$	output function for unit step input function (=unit step response in s domain)
g_{inh} and τ_{inh}	gain and time constant for the unit step response in the inhalation step
g_{art} and τ_{art}	gain and time constant for the unit step response in the arteriolar diffusion step
$\hat{t}$	dimensionless time normalized by t_m
$\hat{r}$	dimensionless radius normalized by r_m
$\hat{c}$	dimensionless concentration $(c-c_A/c_B)$
$\hat{V}$	dimensionless volume $(V-V_A/V_B)$
$D_{NO,w}$	diffusion coefficient of NO in water phase ($\mu m^2\ s^{-1}$)
k_h	rate constant for NO-hemoglobin reaction (s^{-1}).
Da	Damkohler number: $D_{NO,w}/r_{SF}^2 k_h$
h	partition coefficient of NO between gas and aqueous phase
p	period of spike-inhalation (s)
n	breath number

REFERENCES

[1] Bentely, J., D. Rickaby, S. T. Haworth, S. T. Hanger, C. C. Hanger, and C. A. Dawson. Pulmonary arterial dilation by inhaled NO: Arterial diameter, NO concentration relationship. *J. Appl. Physiol.* 91:1948–1954, 2001.

[2] Bird, R. B., W. E. Stewart, and E. N. Lightfoot. Transport Phenomena. New York: Wiley, 1960, p. 46.

[3] Brandish, P. E., W. Buechler, and M. A. Marletta. Regeneration of the ferrous heme of soluble guanylate cyclase from the nitric oxide complex: Acceleration by thiols and oxyhemoglobin. *Biochemistry* 37:16898–16907, 1998.

[4] Butler, A. R., I. L. Megson, and P. G. Wright. Diffusion of nitric oxide and scavenging by blood in the vasculature. *Biochim. Biophys. Acta* 1425:168–176, 1998.

[5] Condorelli, P., and S. C. George. *In vivo* control of soluble guanylate cyclase activation by nitric oxide: A kinetic analysis. *Biophys. J.* 80:2110–2119, 2001.

[6] Cumming, G., and J. G. Jones. The construction and repeatability of nitrogen clearance curves. *Respir. Physiol.* 1:238–248, 1966.

[7] Denninger, J. W., and M. A. Marletta. Guanylyl cyclase and NO/cGMP signaling pathway. *Biochim. Biophys. Acta* 1411:334–350, 1999.

[8] Dierks, E. A., and J. N. Burstyn. The deactivation of soluble guanylyl cyclase by redox-active agents. *Arch. Biochem. Biophys.* 351:1–7, 1998.

[9] Gow, A. J., and J. S. Stamler. Reaction between nitric oxide and haemoglobin under physiological condition. *Nature (London)* 391:169–173, 1998.

[10] Harris, P., and D. Heath. The Human Pulmonary Circulation: Its Form and Function in Health and Disease. New York: Churchill Livingstone, 1977, p. 712.

[11] Higenbottam, T. Pathophysiology of pulmonary hypertension: A role for endothelial dysfunction. *Chest* 105:7S–11S, 1994.

[12] Horsefield, K. Morphometry of the small pulmonary arteries in man. *Circ. Res.* 42:593–597, 1978.

[13] International Critical Tables. New York: McGraw-Hill, 1928, Vol. 3, pp. 255–260.

[14] Jia, L., C. Bonaventura, J. Bonaventura, and J. S. Stamler. S-nitrosohaemoglobin: A dynamic activity of blood involved in vascular control. *Nature (London)* 380:221–226, 1996.

[15] Katayama, Y., T. W. Higenbottam, G. Cremona, S. Akamine, E. A. G. Demoncheaux, A. P. L. Smith, and T. E. Siddons. Minimizing the inhaled dose of NO with breath-by-breath delivery of spikes of concentrated gas. *Circulation* 98:2429–2432, 1998.

[16] Kemming, G. I., M. J. Merkel, A. Schaller, O. P. Habler, M. S. Kleen, M. Haller, J. Briegel, C. Vogelmeier, H. Furst, B. Reichant, and B. Zwissler. Inhaled nitric oxide (NO) for the treatment of early allograft failure after lung transplantation. *Munich Lung Transpl. Group. Intensive Care Med.* 24:1173–1180, 1998.

[17] Kharitonov, V. G., V. J. Sharma, D. Magde, and D. Koesling. Kinetics of nitric oxide dissociation from five- and six-coordinate nitrosyl hemes and heme proteins, including soluble guanylate cyclase. *Biochemistry* 36:6814–6818, 1997.

[18] Liu, X., M. J. S. Miller, M. S. Joshi, H. Sadowska-Krowicka, D. A. Clark, and D. A. Lancaster, Jr. Diffusion-limited reaction of free nitric oxide with erythrocytes. *J. Biol. Chem.* 273:18709–18713, 1998.

[19] Malinski, T., Z. Taha, S. Grunfeld, S. Patton, M. Kapturezak, and P. Tomboulian. Diffusion of nitric oxide in the aorta wall monitored *in situ* by porphyrinic microsensors. *Biochem. Biophys. Res. Commun.* 193:1076–1082, 1993.

[20] Moncada, S., and E. A. Higgs. Molecular mechanisms and therapeutic strategies related to nitric oxide. *Fed. Am. Soc. Exp. Biol.* 9: 1319–1330, 1995.

[21] Moncada, S., R. M. J. Palmer, and E. A. Higgs. Nitric oxide: Physiology, pathphysiology, and pharmacology. *Pharmacol. Rev.* 43:109–142, 1991.

[22] Palevsky, H. I., and A. P. Fishman. The management of primary pulmonary hypertension. *J. Am. Med. Assoc.* 265:1014–1020, 1991.

[23] Reid, L., R. Geggel, R. Fried, and D. Langleben. Anatomy of pulmonary hypertensive states. In: Abnormal Pulmonary Circulation, edited by E. H. Bergofsky. New York: Churchill Livingstone, 1986, pp. 221–239.

[24] Rich, S. The medical treatment of primary pulmonary hypertension. *Chest* 105:17S–19S, 1994.

[25] Rossaint, R., K. J. Fulke, F. Lopez, K. Slama, U. Pison, and W. M. Zapol. Inhaled nitric oxide for the adult respiratory distress syndrome. *N. Engl. J. Med.* 328:399–405, 1993.

[26] Rubanyi, G. M. Endothelium-derived relaxing and contracting factors. *J. Cell. Biochem.* 46: 27–36, 1991.

[27] Stone, J. R., and M. A. Marletta. Spectral and kinetic studies on the activation of soluble guanylate cyclase by nitric oxide. *Biochemistry* 35:1093–1099, 1996.

[28] Taylor, W. E. Pathophysiology of pulmonary heart disease. In: Pulmonary Heart Disease, edited by L. J. Rubin. Boston: Martinus Nijhoff, 1984, pp. 65–105.
[29] Tsoukias, N. M., D. Dabdub, A. F. Wilson, and S. C. George. Effect of alveolar volume and sequential filling on the diffusion capacity of the lungs: II. Experiment. *Respir. Physiol.* 120:251–271, 2000.
[30] Vaughn, M. W., K. Huang, L. Kuo, and J. C. Liao. Erythrocytes possess an intrinsic barrier to nitric oxide consumption. *J. Biol. Chem.* 275:2342–2348, 2000.
[31] Vaughn, M. W., L. Kuo, and J. C. Liao. Effective diffusion distance of nitric oxide in the microcirculation. *Am. J. Physiol.* 274:H1705–H1714, 1998.
[32] Vender, R. L. Chronic hypoxic pulmonary hypertension: Cell biology to pathophysiology. *Chest* 106:236–243, 1994.
[33] Wagenvoort, C. A., and N. Wagenvoort. Pathology of Pumonary Hypertension. New York: Wiley Medical, 1977, p. 345.
[34] Warner, T. M., J. A. Mitchell, H. Sheng, and F. Murad. Effect of cyclic GMP on smooth muscle relaxation. *Adv. Pharmacol.* 26:171–194, 1994.
[35] West, J. B. Respiratory Physiology—The Essentials. Baltimore MD: Williams and Wilkins, 1995, 171 pp.
[36] Wise, D. L., and G. Houghton. Diffusion coefficients of neon, krypton, xenon, carbon monoxide, and nitric oxide in water at 10–60°C. *Chem. Eng. Sci.* 23:1211–1216, 1968.
[37] Zapol, W. M., and W. E. Hurford. Inhaled oxide in adult respiratory distress syndrome and other lung diseases. *Adv. Pharmacol.* 31:513–530, 1994.